On Quaternion Maps with Memory

Ramón Alonso-Sanz
Technical University of Madrid, ETSIA (Estadistica, GSC)
C. Universitaria. 28040, Madrid, Spain
ramon.alonso@upm.es

An exploratory study is made of the dynamics of quaternion iterative maps endowed with memory of past states. Particular attention is paid to the quadratic map.

1. Introduction: Quaternion Maps with Memory

1.1 Quaternions

Quaternions are a class of hypercomplex numbers with four real components [1]. By analogy with the complex numbers being representable as a sum of real and imaginary parts ($z = a + bi$), quaternions can also be written as a linear combination:

$$q = a + bi + cj + dk, \tag{1}$$

where $(1, i, j, k)$ make a group and satisfy the noncommutative rules:

$$i^2 = j^2 = k^2 = -1,\ ij = -ji = k,\ jk = -kj = i,\ ki = -ik = j.$$

The quaternions were introduced in 1843 by W. R. Hamilton. The controversy about them grew in the late 1800s so that, despite Hamilton's supporters, who opposed the growing field of vector algebra, vector notation and calculus largely replaced the "space-time" quaternions in science and engineering by the mid-twentieth century. It has been said that quaternions are a "solution in search of a problem." The reader interested in the historic evolution of the role played by quaternions in science may find particularly interesting [2], which describes its "strange passage from glory to decay," albeit "a number of applications went on appearing from time to time." Thus, quaternions have been used in both theoretical and applied sciences, in particular for calculations involving three-dimensional rotations (and interpolation), alongside other methods, such as Euler angles and rotation matrices, or as an alternative to them, depending on the application. Their capability to succinctly represent three-dimensional rotations about an arbitrary axis has motivated researchers to employ quaternions in rotational kinematics equations. As a result, new applications involving quaternion-based algorithms emerged; these include fields such as robotics, orbital mechanics, aerospace technologies, computer

https://doi.org/10.25088/ComplexSystems.24.3.223

graphics, computer vision and games, animation, and virtual reality [3, 4].

1.2 Discrete Maps with Memory

Conventional *discrete dynamical systems* are memoryless; that is, the next state depends solely on the current one:

$$z_{T+1} = f(z_T).$$

Two seemingly natural ways of implementing an explicit dependence on the dynamics of the past states are:

$$z_{T+1} = f\left(\sum_{t=1}^{T} p_t z_t\right), \tag{2}$$

and

$$z_{T+1} = \sum_{t=1}^{T} p_t f(z_t). \tag{3}$$

The weights p fulfill the probabilistic-like normalization condition $\sum_{t=1}^{T} p_t = 1, p_t \geq 0$. Initially, $z_2 = f(z_1)$ in both scenarios.

The memory implementation given by equation (2) will be referred to as *embedded* memory [5], whereas the memory implementation given by equation (3) will be referred to as *delay* memory.

We have explored the effect of memory on the quadratic complex map $z_{T+1} = z_T^2 + z_c$ in previous work [6–9]. Attention will be paid here to the quaternion quadratic iterative map [10–14]:

$$q_{T+1} = q_T^2 + q_c, \quad q_0 = 0, \quad q_c = (c_r, c_i, c_j, c_k). \tag{4}$$

2. Unlimited Trailing Memory

We will consider first the effect of average memory with geometric decay based on the *memory factor* α lying in the $[0, 1]$ interval:

$$q_{T+1} = \begin{cases} f\left(\dfrac{q_T + \sum_{t=1}^{T-1} \alpha^{T-t} q_t}{\Omega(T)} \equiv \dfrac{\omega(T)}{\Omega(T)} = \dfrac{q_T + \alpha\omega(T-1)}{\Omega(T)}\right) \\ \dfrac{f(q_T) + \sum_{t=1}^{T-1} \alpha^{T-t} f(q_t)}{\Omega(T)} \equiv \dfrac{\omega(T)}{\Omega(T)} = \dfrac{f(q_T) + \alpha\omega(T-1)}{\Omega(T)} \end{cases}, \tag{5}$$

where the first line applies for embedded memory and the second one for delay memory. In both scenarios, Ω stands for the sums of the pondering factors; that is, $\Omega(T) = 1 + \sum_{t=1}^{T-1} \alpha^{T-t}$.

https://doi.org/10.25088/ComplexSystems.24.3.223

The Mandelbrot set is the set of all q_c for which the iterative map (equation (4)), starting from $q = 0$, does not diverge to infinity ([15, 16, Chapter 14]). In the computer implementation here, convergence is assumed if $|q_T| = \sqrt{a_T^2 + b_T^2 + c_T^2 + d_T^2}$ remains below a given δ after a given number of iterations. This is similar to the method in the study of the effect of memory in the complex plane in [7–9].

Figures 1–6 show the effect of memory on the Mandelbrot set, with simulations that run up to either $T = 100$ or divergence, precisely up to $|q|$ reaching the breakout value $\delta = 8.0$. Thus, red indicates the Mandelbrot set, blue indicates divergence at an even time step number, and white indicates divergence at an odd time step number. The region of the complex plane shown in these figures is $[-3.9, 2.5] \times [-3.2, 3.2]$. The graphics shown in Figures 1–6 remain symmetrical around the real axis with memory, as in the conventional scenario.

Figure 1 shows the effect of α-memory on the Mandelbrot set for $c_j = c_k = 0.5$ fixed. Both the embedded and delay memory scenarios are addressed in Figure 1. In both scenarios, as a result induced by the inertial effect that α-memory exerts, $\mathbf{M}$ grows as α increases, though it remains inside the region bounded by the outer blue band (points that diverge at $T = 2$), which, in turn, is not very much altered. The sophisticated aspect of the proximity of $\mathbf{M}$ is fairly preserved with very low memory charge, but tends to vanish as α increases.

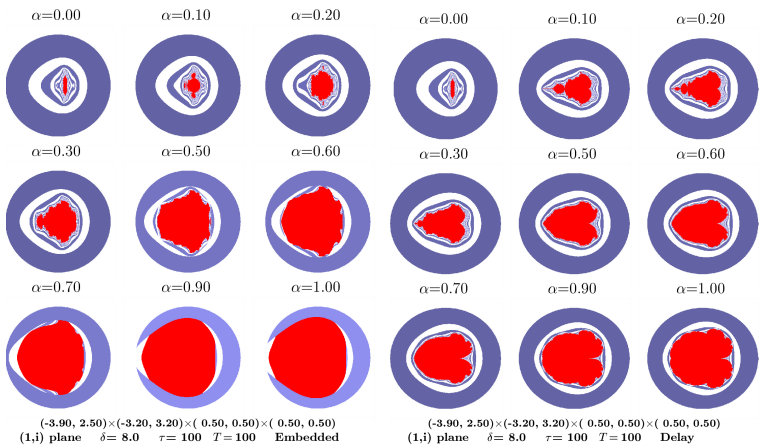

(a) (b)

Figure 1. The Mandelbrot set with unlimited α-memory. $c_j = c_k = 0.5$. (a) Embedded memory. (b) Delay memory.

https://doi.org/10.25088/ComplexSystems.24.3.223

In the ahistoric model of Figure 1, the area of the Mandelbrot set, estimated by pixel counting, turns out as small as 0.175. When increasing α as in Figure 1, the area of the Mandelbrot set grows progressively in the embedded memory scenario as the series 0.558, 1.399, 2.844, 6.367, 10.385, 8.511, 12.851, 13.780; and in the delay memory scenario as the series 0.175, 1.894, 2.488, 3.225, 4.567, 5.249, 5.967, 7.481, 8.240.

The center of gravity of **M** stays in the real axis in all the simulations here. It slowly drifts progressively to lower values in the simulations of Figure 1. The estimation by pixel counting of the real coordinate of the center of gravity evolves as -0.125, -0.227, -0.286, -0.439, -0.636, -0.714, -0.788, -0.871, -0.908; and -0.125, -0.375, -0.430, -0.514, -0.542, -0.540, -0.533, -0.527, -0.525 with embedded and delay memory, respectively.

Figure 2 also shows the effect of unlimited α-memory, but now with $c_j = c_k = 1.0$ instead of $c_j = c_k = 0.5$ as in Figure 1. As a result of such an increase in the levels fixed in the hypercomplex components, the Mandelbrot set turns out empty. In the embedded memory scenario (Figure 2(a)), the Mandelbrot set emerges with $\alpha \geq 0.5$, with much the same appearance as expected in Figure 1. At variance with this, with delay memory (Figure 2(b)), the Mandelbrot set emerges from $\alpha = 0.1$ and adopts a fairly curious aspect.

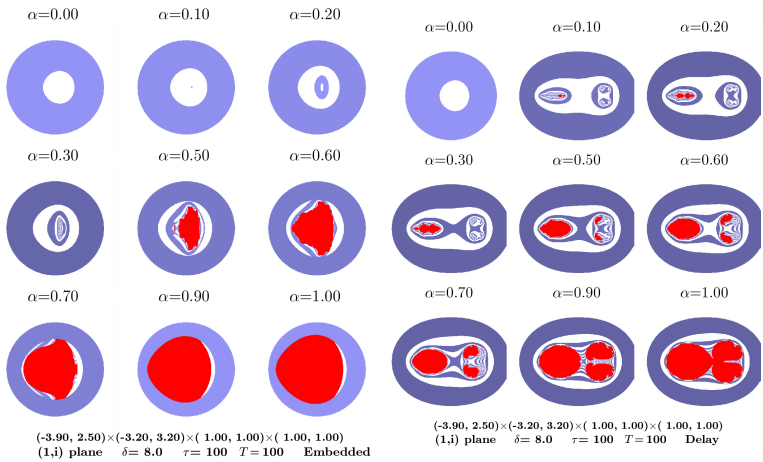

(a) (b)

Figure 2. The Mandelbrot set with unlimited α-memory. $c_j = c_k = 1.0$. (a) Embedded memory. (b) Delay memory.

https://doi.org/10.25088/ComplexSystems.24.3.223

3. Limited Trailing Memory

Limited trailing memory would keep a memory of only the last τ time steps. Thus:

$$q_{T+1} = \begin{cases} f\left(\sum_{t=\tau}^{T} \delta_t q_t\right) \\ \sum_{t=\tau}^{T} \delta_t f(q_t) \end{cases},$$

with $\tau = \max\left(1, T - \tau + 1\right)$.

Limiting the trailing memory would make the model approach the ahistoric model $\left(\tau = 1\right)$.

In the geometric decay memory type of equation (5), the lower memory charge is achieved with $\tau = 2$:

$$q_{T+1} = \begin{cases} f\left(\dfrac{q_T + \alpha q_{T-1}}{1 + \alpha}\right) \\ \dfrac{f(q_T) + \alpha f(q_{T-1})}{1 + \alpha} \end{cases}. \tag{6}$$

This kind of memory implementation will be referred to as $\tau = 2$ α-memory.

We will also consider memory of only the last two states implemented in the general form $\left(0 \le \epsilon \le 1\right)$:

$$q_{T+1} = \begin{cases} f\left(\left(1 - \epsilon\right)q_T + \epsilon q_{T-1}\right)\right) \\ \left(1 - \epsilon\right)f(q_T) + \epsilon f(q_{T-1}) \end{cases}. \tag{7}$$

Figure 3 shows the effect of $\tau = 2$ α-memory on the Mandelbrot set. The outer blue band is not appreciably altered in Figure 3(b) (delay memory), much as it was not with unlimited memory in Figure 1. With embedded memory (Figure 3(a)), an appreciable alteration of the outer band is found. In both scenarios, the proximity of **M** to $\tau = 2$ α-memory increases its sophisticated aspect as memory increases. The area of the Mandelbrot set in Figure 3 increases with memory, but not to such a large extent as with unlimited trailing memory. The corresponding series of the area values are 0.175, 0.484, 1.106, 1.837, 3.279, 3.473, 3.311, 2.330, 2.047 (embedded memory); 0.175, 0.414, 0.868, 1.275, 2.173, 2.373, 2.346, 2.138, 1.966 (delay memory). The real coordinate of the center of gravity drifts to the left in Figure 3 as -0.125, -0.226, -0.311, -0.505, -0.784, -0.818, -0.824, -0.596, -0.542 (embedded memory); -0.125, -0.212, -0.270, -0.336, -0.488, -0.516, -0.565, -0.569, -0.541 (delay memory).

A magnification of Figure 3 in the $\left[-1.0, 1.0\right]\times\left[0.0, 2.0\right]$ region is shown in Figure 4. The vicinity of M with $\tau = 2$ α-memory becomes

https://doi.org/10.25088/ComplexSystems.24.3.223

increasingly intricate with memory. Detailed study of magnified views with different memory implementations is due.

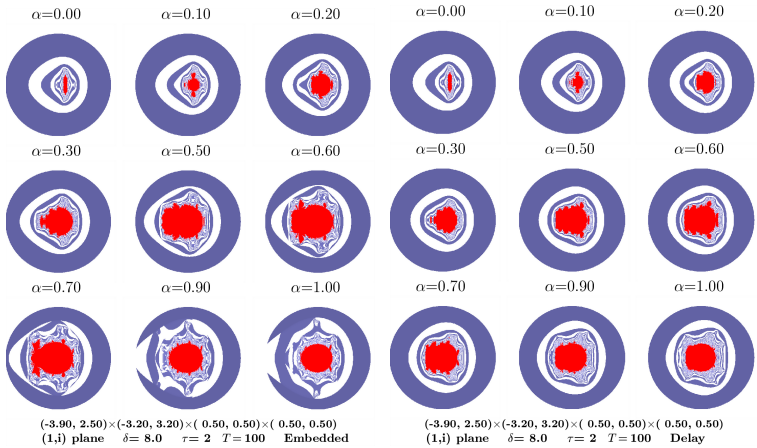

Figure 3. The Mandelbrot set with $\tau = 2$ α-memory. $c_j = c_k = 0.5$. (a) Embedded memory. (b) Delay memory.

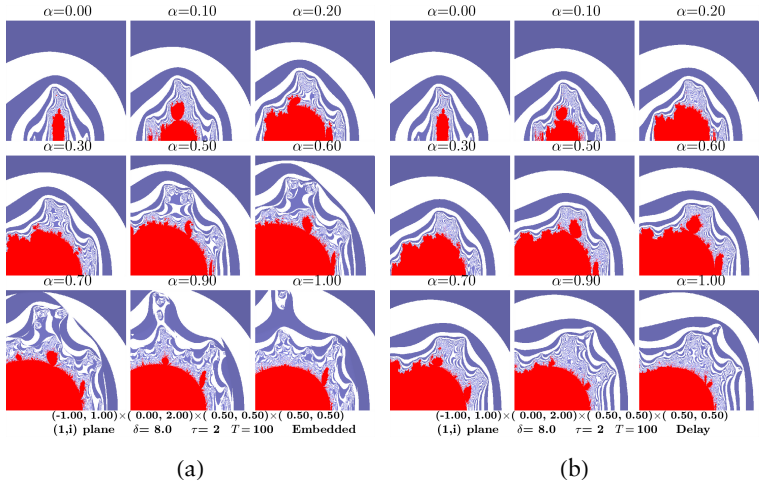

Figure 4. Zoom of Figure 3 in the $[-1.0, 1.0]\times[0.0, 2.0]$ region of the complex plane.

Figure 5 shows the effect of $\tau = 2$ α-memory for fixed $c_j = c_k = 1.0$. The same high levels of the hypercomplex components

https://doi.org/10.25088/ComplexSystems.24.3.223

of Figure 2 are fixed in Figure 5, but the short range (only $\tau = 2$) of the trailing memory implemented in Figure 5 disables the capacity for the Mandelbrot set to emerge as in the unlimited trailing memory scenario of Figure 2.

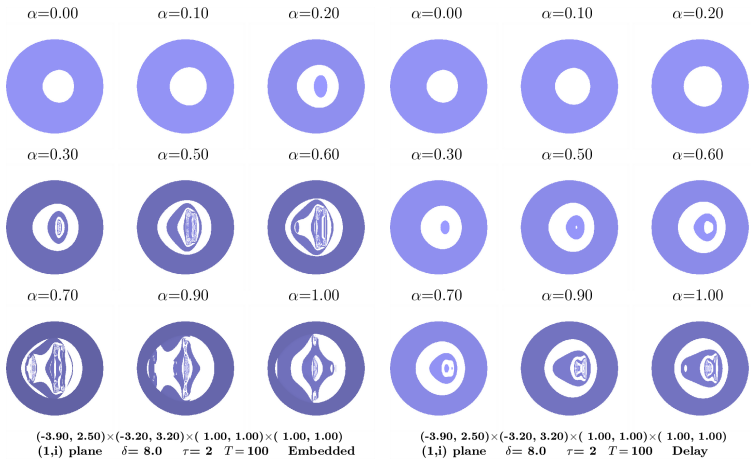

(a) (b)

Figure 5. The Mandelbrot set with $\tau = 2$ α-memory. $c_j = c_k = 1.0$. (a) Embedded memory. (b) Delay memory.

Figure 6 shows the effect of ϵ-memory on the Mandelbrot set. In both scenarios, the outer blue band is highly altered in Figure 6, tending to vanish as the memory factor increases. The Mandelbrot set is appreciably altered by ϵ-memory up to $\epsilon = 0.70$, but tends to recover the original configuration for higher values of ϵ. The scenario of $\epsilon = 0.5$ coincides with that of $\tau = 2$ $\alpha = 1.0$-memory, as can be checked here in Figures 3 and 6. In parallel to the effect of ϵ-memory on $\mathbf{M}$ itself, the sophisticated aspect of the proximity of $\mathbf{M}$ is fairly preserved up to $\epsilon = 0.80$ but shrinks with higher values of ϵ and fairly disappears with $\epsilon = 0.95$. The area of the Mandelbrot set in Figure 6 evolves as 0.175, 2.047, 1.643, 1.303, 1.025, 0.726, 0.358, 0.131, 0.1444 (embedded memory); 0.175, 1.966, 1.586, 1.219, 0.956, 0.688, 0.344, 0.121, 0.1444 (delay memory). The real coordinate of the center of gravity of $\mathbf{M}$ evolves in Figure 6 as -0.125, -0.542, -0.464, -0.398, -0.358, -0.293, -0.220, -0.101, -0.097 (embedded memory); -0.125, -0.541, -0.452, -0.380, -0.342, -0.275, -0.224, -0.096, -0.097 (delay memory).

https://doi.org/10.25088/ComplexSystems.24.3.223

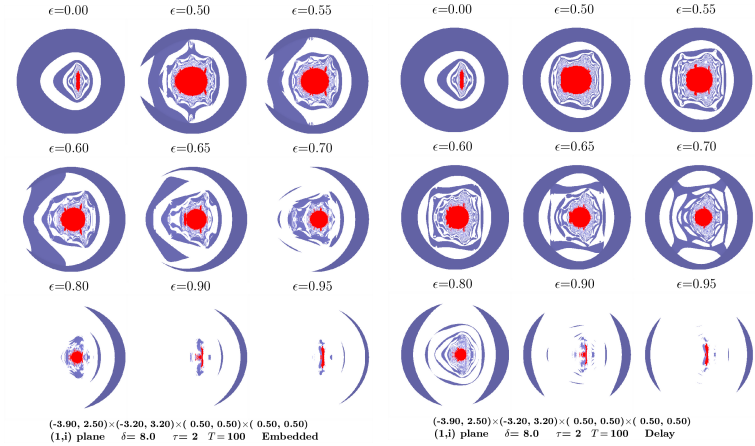

(a) (b)

Figure 6. The Mandelbrot set with ϵ-memory. $c_j = c_k = 0.5$. (a) Embedded memory. (b) Delay memory.

3.1 Partial Memory

The quaternion quadratic map equation (4) is equivalent to the four-dimensional real map:

$$a_{T+1} = a_T^2 - \left(b_T^2 + c_T^2 + d_T^2\right) + c_r \tag{8a}$$
$$b_{T+1} = 2a_T b_T + c_i \tag{8b}$$
$$c_{T+1} = 2a_T c_T + c_j \tag{8c}$$
$$d_{T+1} = 2a_T d_T + c_k \tag{8d}$$

The dynamics defined by equations (8) may then be partially endowed with memory in its coordinates. For example, with embedded memory only in the *real a* component it would be:

$$a_{T+1} = \overline{a}_T^2 - \left(b_T^2 + c_T^2 + d_T^2\right) + c_r$$
$$b_{T+1} = 2\overline{a}_T b_T + c_i$$
$$c_{T+1} = 2\overline{a}_T c_T + c_j$$
$$d_{T+1} = 2\overline{a}_T d_T + c_k$$

with $\overline{a}_T$ denoting a summary of the values of a up to time step T. Thus,

$$\overline{a}_T = \frac{a_T + \sum_{t=1}^{T-1} \alpha^{T-t} a_t}{\Omega(T)}$$

in the unlimited α-memory scenario, and $\overline{a}_T = (1-\epsilon)a_T + \epsilon a_{T-1}$ in the ϵ-memory scenario. Partial memory induces peculiar alterations in the

https://doi.org/10.25088/ComplexSystems.24.3.223

Mandelbrot set (see [8] regarding the complex plane). They are not presented here to avoid increasing the number of images in this paper.

4. Conclusion and Future Work

This paper provides an exploratory study on the effect of memory of the past states on the dynamics of quaternion quadratic iterative maps. Two-dimensional projections of the Mandelbrot set on the hypercomplex components of the quaternion space have been scrutinized in order to assess the effect of memory in a fairly qualitative manner.

Further study of the effect of memory on quaternion maps is due. Two possible areas of study are (1) a more detailed scrutiny of the geometry; and (2) mathematical foundation. In the area of geometry, three-dimensional visualization tools [17–23] implementing ad hoc rendering techniques (as in [24] and [25]) are to be enriched to deal with memory. The second task does not seem easy: adding memory to nonlinear dynamics in the hypercomplex space. Let us point out that fractional calculus has been applied in the analysis of discrete maps with memory [26]. Fractional calculus extends the definition of derivative and integral, allowing for noninteger orders. Thus, the integral of order α, according to the Riemann–Liouville approach, is calculated in the time-domain as

$$D^{\alpha}f(T) = \frac{1}{\Gamma(\alpha)}\int_0^T (T-t)^{\alpha-1} f(t)dt. \tag{9}$$

Rewriting equation (5) (supposing $\alpha > 0$) as:

$$q_{T+1} = \frac{1}{\Omega(\alpha, T)}\sum_{t=1}^{T} \alpha^{T-t} f(q_t), \tag{10}$$

the structure of equation (10) is reminiscent of that of equation (9), which is central to the application of fractional calculus to the study of systems with memory.

Quaternion maps have been used as a tool for modeling in several contexts, for example, in protein structure analysis [27] and in fundamental physics [28]. The potential applicability of the quaternion maps with memory is to be explored in subsequent studies.

Acknowledgment

This work was supported by the Spanish Project M2012-39101-C02-01.

https://doi.org/10.25088/ComplexSystems.24.3.223

References

[1] J. H. Conway and D. A. Smith, *On Quaternions and Octonions: Their Geometry, Arithmetic, and Symmetry*, Natick, MA: A. K. Peters, 2003.

[2] S. L. Altmann, "Hamilton, Rodrigues, and the Quaternion Scandal," *Mathematics Magazine*, **62**(5), 1989 pp. 291–308. doi:10.2307/2689481.

[3] R. Mukundan, "Quaternions: From Classical Mechanics to Computer Graphics and Beyond," in *Proceedings of the 7th Asian Technology Conference in Mathematics (ATCM2002)*, Malacca, Malaysia (W-C. Yang, T. de Alwis, S-C. Chu, and F. M. Bhatti, eds.), ATCM, Inc.: USA, 2002 pp. 97–106. http://epatcm.any2any.us/EP/EP2002/ATCMA107/fullpaper.pdf.

[4] K. Shoemake, "Animating Rotation with Quaternion Curves," in *Proceedings of the 12th Annual Conference on Computer Graphics and Interactive Techniques (SIGGRAPH'85)*, San Francisco, CA, New York: ACM, 1985 pp. 245–254. doi:10.1145/325165.325242.

[5] R. Alonso-Sanz, *Discrete Systems with Memory*, Hackensack, NJ: World Scientific, 2011.

[6] R. Alonso-Sanz, "On Complex Maps with Delay Memory," *Fractals*, forthcoming.

[7] R. Alonso-Sanz, "Scouting the Mandelbrot Set with Memory," *Complexity*, 2014. doi:10.1002/cplx.21632.

[8] R. Alonso-Sanz, "The Mandelbrot Set with Partial Memory," *Complex Systems*, **23**(3), 2014 pp. 227–238. http://www.complex-systems.com/pdf/23-3-2.pdf.

[9] R. Alonso-Sanz, "A Glimpse of Complex Maps with Memory," *Complex Systems*, **21**(4), 2013 pp. 269–282. http://www.complex-systems.com/pdf/21-4-2.pdf.

[10] S. Bedding and K. Briggs, "Iteration of Quaternion Maps," *International Journal of Bifurcation and Chaos*, **5**(3), 1995 pp. 877–881. doi:10.1142/S0218127495000661.

[11] S. Bedding and K. Briggs, "Iteration of Quaternion Functions," *The American Mathematical Monthly*, **103**(8), 1996 pp. 654–664. doi:10.2307/2974877.

[12] J. Gomatam, J. Doyle, B. Steves, and I. McFarlane, "Generalization of the Mandelbrot Set: Quaternionic Quadratic Maps," *Chaos, Solitons & Fractals*, **5**(6), 1995 pp. 971–986. doi:10.1016/0960-0779(94)00163-K.

[13] S. Nakane, "Dynamics of a Family of Quadratic Maps in the Quaternion Space," *International Journal of Bifurcation and Chaos*, **15**(8), 2005 pp. 2535–2543. doi:10.1142/S0218127405013460.

https://doi.org/10.25088/ComplexSystems.24.3.223

[14] X-Y. Wang and Y-Y. Sun, "The General Quaternionic M–J Sets on the Mapping $z \leftarrow z^{\alpha} + c(\alpha \in N)$," *Computers and Mathematics with Applications*, **53**(11), 2007 pp. 1718–1732. doi:10.1016/j.camwa.2007.01.014.

[15] B. B. Mandelbrot, *The Fractal Geometry of Nature*, New York: W. H. Freeman, 1983.

[16] H-O. Peitgen, H. Jürgens, and D. Saupe, *Chaos and Fractals: New Frontiers of Science*, 2nd ed., New York: Springer, 2004.

[17] J. Barrallo, "Expanding the Mandelbrot Set into Higher Dimensions," in *Proceedings of Bridges 2010: Mathematics, Music, Art, Architecture, Culture,* Pecs, Hungary (G. W. Hart and R. Sarganhi, eds.), Phoenix: Tessellations Publishing, 2010 pp. 247–254.

[18] A. J. Hanson, *Visualizing Quaternions*, San Francisco: Morgan Kaufmann, 2006.

[19] J. C. Hart, D. J. Sandin, and L. H. Kaufmann, "Ray Tracing Deterministic 3-D Fractals," in *Proceedings of the 16th Annual Conference on Computer Graphics and Interactive Techniques (SIGGRAPH '89)*, Boston, MA, New York: ACM, 1989 pp. 289–296. doi:10.1145/74333.74363.

[20] A. Norton, "Julia Sets in the Quaternions," *Computers & Graphics*, **13**(2), 1989 pp. 267–278. doi:10.1016/0097-8493(89)90071-X.

[21] H-O. Peitgen and D. Saupe, eds., *The Science of Fractal Images*, New York: Springer-Verlag, 1988.

[22] C. A. Pickover, *Computers, Pattern, Chaos and Beauty: Graphics from an Unseen World*, Mineola, NY: Dover Publications, 2001.

[23] A. Rosa, "Methods and Applications to Display Quaternion Julia Sets," *Differential Equations and Control Processes*, **4**, 2005, http://www.math.spbu.ru/diffjournal/pdf/rosa2.pdf.

[24] I. Quilez. *3D Quaternionic Julia Set–Metallic* [Video]. (Jul 20, 2015) http://www.youtube.com/watch?v=-Siv_jhSkUE.

[25] F. Klingener. "Quaternion Julia Set" from the Wolfram Demonstrations Project—A Wolfram Web Resource. http://demonstrations.wolfram.com/QuaternionJuliaSet.

[26] V. E. Tarasov, *Fractional Dynamics: Applications of Fractional Calculus to Dynamics of Particles, Fields, and Media*, London: Springer, 2010.

[27] A. J. Hanson and S. Thakur, "Quaternion Maps of Global Protein Structure," *Journal of Molecular Graphics and Modelling*, **38**, 2012, pp. 256–278. doi:10.1016/j.jmgm.2012.06.004.

[28] M. P. Mehta, S. Duttab, and S. Tiwari, "A Quaternionic Map for the Steady States of the Heisenberg Spin-Chain," *Physics Letters A*, **378**(4), 2014 pp. 362–366. doi:10.1016/j.physleta.2013.11.032.

https://doi.org/10.25088/ComplexSystems.24.3.223